Deprivation-induced synaptic depression by distinct mechanisms in different layers of mouse visual cortex

Robert A. Crozier*†, Yun Wang‡, Cheng-Hang Liu*, and Mark F. Bear*§

*Howard Hughes Medical Institute, The Picower Institute for Learning and Memory, Department of Brain and Cognitive Science, Massachusetts Institute of Technology, 177 Massachusetts Avenue, Cambridge, MA 02139; and ‡Division of Neurology Research, Caritas St. Elizabeth's Medical Center, Tufts University, Boston, MA 02135

Edited by Richard L. Huganir, Johns Hopkins University School of Medicine, Baltimore, MD, and approved November 28, 2006 (received for review October 28, 2006)

Long-term depression (LTD) induced by low-frequency synaptic stimulation (LFS) was originally introduced as a model to probe potential mechanisms of deprivation-induced synaptic depression in visual cortex. In hippocampus, LTD requires activation of postsynaptic NMDA receptors, PKA, and the clathrin-dependent endocytosis of α-amino-3-hydroxy-5-methyl-4-isoxazolepropionic acid (AMPA) receptors. It has long been assumed that LTD induced in visual cortical layer 2/3 by LFS of layer 4 uses similar mechanisms. Here we show in mouse visual cortex that this conclusion requires revision. We find that LTD induced in layer 2/3 by LFS is unaffected by inhibitors of PKA or α-amino-3-hydroxy-5-methyl-4-isoxazolepropionic acid receptor endocytosis but is reliably blocked by an endocannabinoid CB1 receptor antagonist. Conversely, LFS applied to synapses on layer 4 neurons produces LTD that appears mechanistically identical to that in CA1 and is insensitive to CB1 blockers. Occlusion experiments suggest that both mechanisms contribute to the loss of visual responsiveness after monocular deprivation.

endocannabinoid | glutamate receptor | long-term depression | ocular dominance plasticity

For decades, neuroscientists have sought to understand how brief monocular deprivation (MD) in early life causes a loss of visual responsiveness in visual cortex that results in amblyopia. The laminar structure of the neocortex has allowed researchers to investigate the mechanisms of synaptic depression both *in vivo* and *in vitro* in a layer-specific manner. The feed-forward circuit is as follows: thalamus → layer 4 → layer 2/3 → layer 5 (1). Long-term depression (LTD) of synaptic responses in visual cortical layer 2/3 induced by low-frequency stimulation (LFS) of layer 4 is a widely studied phenomenon that is believed to share mechanisms with those that cause synaptic depression after MD (2). Based on similar frequency and NMDA receptor (NMDAR) dependence, it has long been assumed that mechanisms of layer 2/3 LTD are the same as those in area CA1 of the hippocampus (3, 4), which involve postsynaptic calcium flux through NMDARs, dephosphorylation of postsynaptic PKA substrates, and clathrin-dependent internalization of α-amino-3-hydroxy-5-methyl-4-isoxazolepropionic acid (AMPA) receptors (AMPARs; ref. 5). Indeed, MD produces changes in AMPAR phosphorylation and surface expression in rat visual cortex that mimic CA1 LTD (6).

In the meantime, a protocol for the induction of LTD by precisely timed pre- and postsynaptic action potentials has gained popularity (7). That spike-timing-dependent LTD (STD-LTD), like LFS-dependent LTD (LFS-LTD), is also blocked by bath application of an NMDAR antagonist initially suggested that common mechanisms are engaged by the two types of induction protocol (8). However, this notion was soon challenged by evidence that STD-LTD in layer 5 neurons from neonatal visual cortex depends on endocannabinoid signaling and pre- rather than postsynaptic NMDAR activation (9).

These interesting findings compelled us to reexamine with greater precision the question of how LFS induces NMDAR-dependent LTD in the radial excitatory pathways of visual cortex. This issue is of considerable significance, because CA1 LTD has been used to inform hypotheses about the molecular basis of ocular dominance plasticity (2, 6). We performed this study in mouse visual cortex, because this has emerged as a favored preparation to study the mechanisms of ocular dominance plasticity *in vivo*. LFS-LTD induced in layer 4 by white-matter stimulation was compared with LFS-LTD induced in layer 2/3 by layer 4 stimulation. We found that identical LFS protocols induce comparable LTD in both locations by activation of postsynaptic NMDARs, as expected. To our surprise, however, we found that the mechanism of layer 2/3 LTD is qualitatively different from that of CA1 and requires activation of cannabinoid receptors. On the other hand, layer 4 LTD is very similar to that of CA1, notably including sensitivity to inhibitors of PKA and AMPAR endocytosis. We further found that both types of LTD are reduced in visual cortex after a period of MD *in vivo*.

Together, our results show that LTD induced by identical stimulation protocols in mouse visual cortex depends on distinct mechanisms in layers 3 and 4. Because deprivation-induced synaptic depression *in vivo* occludes both types of LTD, our findings strongly suggest that different mechanisms contribute to the effects of MD in different layers of mouse visual cortex.

Results

Reliable LTD Expression in Layers 3 and 4. We first sought to establish that LTD could be induced with an LFS protocol in both layers 2/3 and 4. Somatic whole-cell voltage-clamp recordings were obtained from pyramidal neurons in either layer in slices prepared from mice at postnatal day (P)21–28. Excitatory postsynaptic currents (EPSCs) were elicited in layer 2/3 by layer 4 stimulation or in layer 4 by white-matter stimulation (just below layer 6). After achieving a stable baseline, repeated brief postsynaptic depolarizations were paired with LFS to induce LTD (Fig. 1). This protocol reliably induced LTD in layer 2/3 (EPSC amplitude after LFS = 65.7 ± 2.6% of baseline, $n = 5$; Fig. 1*a*). In layer 4, previous reports suggested considerable variability in the ability to induce LTD with LFS (compare refs. 4 and 10). However, we found that our pairing protocol also reliably induced LTD in layer 4 (71.5 ± 8.1% of baseline, $n = 5$; Fig. 1*b*).

Author contributions: R.A.C., Y.W., C.-H.L., and M.F.B. designed research; R.A.C., Y.W., and C.-H.L. performed research; R.A.C. and M.F.B. analyzed data; and R.A.C. and M.F.B. wrote the paper.

The authors declare no conflict of interest.

This article is a PNAS direct submission.

Abbreviations: LFS, low-frequency stimulation; LTD, long-term depression; STD-LTD, spike-timing-dependent LTD; EPSC, excitatory postsynaptic current; EPSP, excitatory postsynaptic potential; AMPA, α-amino-3-hydroxy-5-methyl-4-isoxazolepropionic acid; AMPAR, AMPA receptor; MD, monocular deprivation; NMDAR, NMDA receptor; P*n*, postnatal day *n*; APV, DL-2-amino-5-phosphonovalerate.

†Present address: Wyeth Research, Discovery Neuroscience, CN8000, Princeton, NJ 08543.

§To whom correspondence should be addressed. E-mail: mbear@mit.edu.

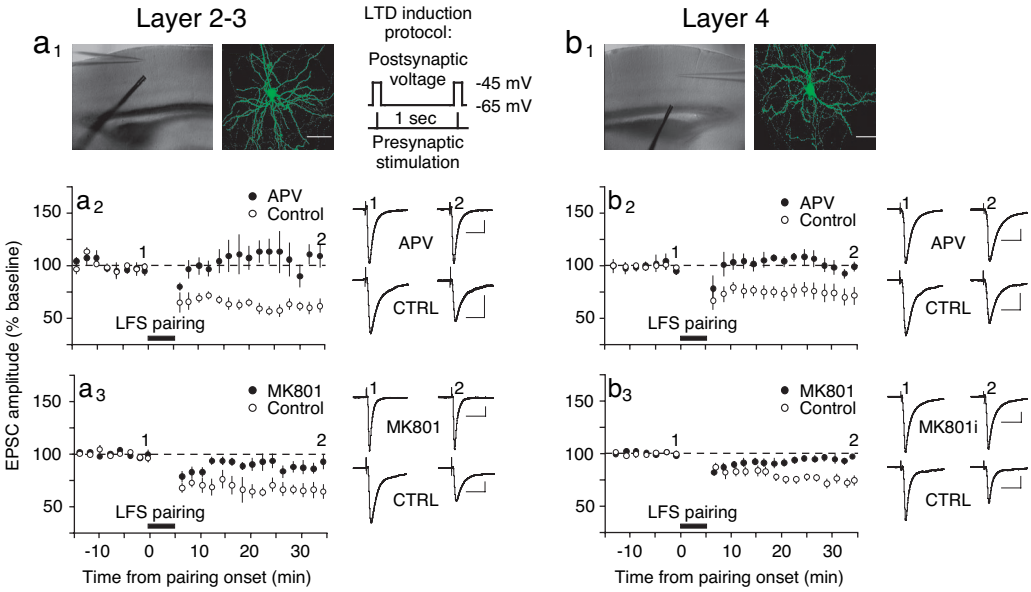

Fig. 1. Similarities in pairing-induced LTD in layers 4 and 3 of mouse visual cortex. (*a* and *b*) Displayed are grouped data time courses and representative sweeps from layers 2/3 (*a*) and 4 (*b*) recordings. (a_1 and b_1) Differential interference contrast images of typical recording configurations and confocal images of neurons filled with biocytin and subsequently detected with streptavidin. (a_1) Schematic illustration of the pairing protocol used to induce LTD: 20-mV, 100-msec postsynaptic step depolarizations paired with 1-Hz presynaptic stimulation that occur halfway (50 msec) into step depolarization. (a_2 and b_2) Control recordings from layer 2/3 (a_2) or layer 4 (b_2) demonstrate that LTD can be observed in either layer. Bath application of APV (100 μM) prevents LTD in both layers. (a_3 and b_3) Intracellular loading of the NMDAR antagonist MK801 (500 μM) by the recording pipette largely blocked LTD in both layers. The *y* axis is EPSC amplitude normalized to a 15-min baseline period with error bars indicating the SEM. The pairing protocol, denoted by black bar, was administered at time 0 and lasted 5 min. The dashed horizontal line indicates no change from baseline responses. Sweep numbers (1, 2) refer to averaged responses collected during the last 5 min of the baseline and postpairing periods. Stimulation artifacts were minimized for clarity. (Scale bars: a_1 and b_1; 50 μm; a_2, a_3, b_2, and b_3, 50 pA and 20 msec.) See Fig. 4 for statistical comparisons.

Mechanistic Similarities in LTD Between Layers 2/3 and 4. We then asked whether LTD in both layers was similarly NMDAR-dependent. As expected from previous work (3, 4, 11), LTD in layer 2/3 was prevented by bath-applied 100 μM DL-2-amino-5-phosphonovalerate (APV). EPSC amplitude after LFS was 106.7 ± 9.2% of baseline in the presence of APV ($n = 5$, Fig. 1a_1). Similarly, APV blocked LTD in layer 4 (97.3 ± 3.1% of baseline, $n = 3$, Fig. 1b_1). To disambiguate the role of pre- vs. postsynaptic NMDAR in layers 2/3 and 4, we loaded individual neurons with MK801 (500 μM), which can block postsynaptic NMDAR channels intracellularly (12–15). We found that LTD was almost entirely blocked by intracellular MK801 in layers 2/3 (91.2 ± 6.3% of baseline, $n = 6$, Fig. 1a_2) and 4 (94.3 ± 2.8% of baseline, $n = 7$, Fig. 1b_2). Interleaved control recordings yielded robust LTD in both layers (layer 2/3, 65.5 ± 6.2%, $n = 5$; layer 4, 73.8 ± 3.9%, $n = 6$).

To ensure that MK801 introduced postsynaptically does not leak out to affect presynaptic NMDAR, we studied STD-LTD in layer 3 of juvenile mice, which, like STD-LTD in layer 5 (9), is sensitive to blockade of pre- but not postsynaptic NMDARs (15). In contrast to LFS-LTD and in support of those prior studies, blocking postsynaptic NMDARs with 500 μM MK801 intracellularly did not prevent STD-LTD [excitatory postsynaptic potential (EPSP) amplitude, 62.4 ± 11.9%; slope, 62.4 ± 15.3%, $n = 7$; Fig. 2]. However, bath-applied APV prevented STD-LTD (EPSP amplitude, 95.5 ± 6.7%; slope, 99.1 ± 13.9%, $n = 7$).

In addition to confirming that STD-LTD is insensitive to blockade of postsynaptic NMDARs, these experiments show that MK801 applied intracellularly does not leak out to affect presynaptic NMDARs, in which case the effect of MK801 on STD-LTD would be identical to bath-applied APV. Together, the data suggest that the induction of LTD by identical LFS protocols in both layers 2/3 and 4 requires postsynaptic NMDAR activation.

Mechanistic Differences in LTD Between Layers 2/3 and 4. The dependence on postsynaptic NMDAR activation for LFS-LTD in both layers 2/3 and 4 of mouse visual cortex allows specific predictions about the molecular cascades stimulated by calcium influx through NMDARs, based on work performed in CA1. Consistent findings in CA1 are inhibition of LTD by blockers of PKA and AMPAR endocytosis. Therefore, we next performed intracellular loading experiments, using either the selective PKA inhibitor PKI (6–22 amide; 10 μM) or a peptide (termed G2CT; 10 μM, KRMKLNINPS) that competes with endogenous GluR2 for the AP2 clathrin adaptor complex and blocks AMPAR endocytosis (16).

We were very surprised to find that the magnitude of LTD in layer 2/3 cells loaded with PKI (66.6 ± 7.6%, $n = 4$; Fig. 3a_2) was indistinguishable from LTD in interleaved control experiments (67.7 ± 8.3%, $n = 5$). Similarly, loading neurons with the G2CT peptide had no effect on LTD in layer 2/3 (70.4 ± 4.8%, $n = 7$, vs. interleaved control LTD, 68.8 ± 2.4%, $n = 6$; Fig. 3a_3). However, the same reagents loaded into layer 4 neurons strongly blocked LTD induced by the same induction protocol. LTD in layer 4 was almost completely prevented by PKI (PKI, 94.1 ± 5.1%, $n = 5$; control, 74.8 ± 5.3%, $n = 7$; Fig. 3b_2). Similarly, loading the G2CT peptide into layer 4 neurons had no effect on basal transmission but strongly inhibited LTD (G2CT, 93.5 ± 4.0%, $n = 7$; control, 69.0 ± 4.1%, $n = 6$; Fig. 3b_3).

These results suggest that LTD induced in layer 4 by stimulating radial inputs involves the PKA-regulated endocytosis of GluR2-containing AMPARs, as has been proposed for CA1. However, what could account for the NMDAR-dependent LTD in layer 2/3? Studies of STD-LTD between pairs of visual cortex layer 5 neurons first revealed a potential mechanism involving retrograde endocannabinoid signaling by presynaptic CB1 receptors (9). The possibility that this mechanism could also contribute to LTD in layer 2/3 was also recently suggested by studies in rat barrel cortex (15). We therefore investigated the effect of the highly potent CB1 receptor antagonist AM251 (2

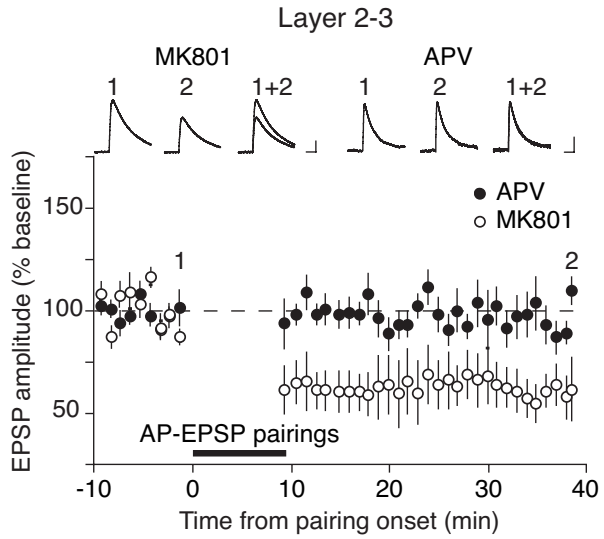

Fig. 2. Spike-timing LTD is insensitive to postsynaptic NMDAR blockade. Displayed are grouped data time courses and representative sweeps from whole-cell current-clamp recordings examining STD-LTD from visual cortex slices obtained from P13–P15 mice (15). In contrast to LFS-LTD, cells loaded with MK801 manifested robust STD-LTD (EPSP amplitude, 62.4 ± 11.9%; slope, 62.4 ± 15.3%; $n = 7$), whereas bath application of APV prevented STD-LTD (EPSP amplitude, 95.5 ± 6.7%; slope, 99.1 ± 13.9%; $n = 7$). 1 and 2 indicate 5-min periods for the averaging of EPSPs just before pairing (1) or at the conclusion of the recording session (2). Stimulus artifacts were minimized for clarity. (Scale bar: 1 mV, 10 msec.) The dashed line indicates no change from baseline responses.

μM) on LTD in layers 3 and 4. The results were complementary to what we found with PKI and the G2CT peptide; inhibition of LTD in layer 2/3 without any effect on LTD in layer 4 (Fig. 3 a_4 and b_4). Layer 2/3 LTD in the presence of AM251 was 88.8 ± 8.3% of control ($n = 6$) vs. the interleaved control LTD measuring 70.8 ± 6.5% of baseline ($n = 5$). In contrast, layer 4 LTD in the presence of AM251 (79.9 ± 3.4% of baseline, $n = 7$) was the same as in the interleaved controls (78.1 ± 7.1% of baseline, $n = 6$).

Because of our interest in comparing LTD in layers 3 and 4, we routinely used whole-cell voltage clamp. However, LTD in layer 2/3 is often studied by using field-potential (FP) recordings. To confirm that our findings were not peculiar to the method used to induce or record LFS-LTD, we performed additional experiments using FP recordings. Because we cannot provide intracellular depolarization during LFS, LTD using FPs requires a longer LFS period (15 min). Nonetheless, layer 2/3 LTD was again strongly inhibited by AM251 (92.0 ± 3.3% of baseline, $n = 7$) compared with interleaved controls (76.3 ± 6.6% of baseline, $n = 7$; $P < 0.05$; data not shown).

Fig. 4 summarizes the whole-cell voltage-clamp recordings of the similarities and differences in LTD induced by the same stimulation protocol in the two layers and provides the necessary statistical comparisons, which, we note, are always made with interleaved controls. Significant inhibition of LTD was achieved in both layers by bath APV and intracellular MK801. Although there was no significant effect of PKI or the G2CT peptide in layer 2/3, both reagents produced significant block in layer 4. In contrast, AM251 was without effect in layer 4 but produced significant block in layer 2/3. These results indicate that the paths leading to LTD diverge according to cell or synapse type, despite the common induction protocol and requirement for postsynaptic NMDAR activation.

Occlusion of LTD in Layers 3 and 4 by Previous MD. These findings, considered with an earlier report of differences in LTD induction requirements in the superficial and deep layers of rat visual cortex (4) potentially impact the conclusion that MD induces CA1-type LTD in visual cortex *in vivo* (6). That conclusion, from a study of rat visual cortex, was supported by two main lines of evidence. First, it was found that MD mimics LTD with respect to depressed synaptic transmission, altered AMPAR phosphorylation, and decreased AMPAR surface expression. Second, it was found that synaptic depression caused by MD occludes LTD in layer 2/3 studied *ex vivo*. However, the current findings in mice suggest that occlusion of LTD in layer 2/3 may not adequately address the question of whether AMPAR internalization is a mechanism for ocular dominance plasticity. Therefore, we thought it was important to reexamine the effect of MD *in vivo* on the CA1-type LTD in layer 4 and the CB1-mediated LTD in layer 2/3 in mouse visual cortex *ex vivo*.

Mice were monocularly deprived at P28 for 3 days, a duration that produces maximal depression of visually evoked potentials recorded from layer 4 *in vivo* (17) without inducing metaplasticity, which could alter the induction requirements for LTD (18). On the third day, slices were prepared from visual cortex contralateral and ipsilateral to the deprived eye. Rodents show an interhemispheric asymmetry in the effect of MD; visual responses in the cortex contralateral to the deprived eye are depressed relative to the ipsilateral hemisphere (6). Thus, the contralateral hemisphere can be viewed as "deprived" relative to the same-animal ipsilateral "control" hemisphere.

With the experimenter blind to the visual history of the mice from which slices were obtained, whole-cell voltage-clamp recordings were performed from layer 4 neurons from the binocular zone of each hemisphere. LTD was induced with the same pairing protocol but for twice the duration as the previous recordings, to saturate the magnitude of LTD. That we observed no further depression after doubling the number of stimuli in control (nondeprived) slices confirmed that LTD is saturated and, further, that extended stimulation does not recruit alternate (e.g., CB1-dependent) mechanisms of LTD (compare Figs. 1 and 4). The results clearly showed that LTD at saturation is reduced in the hemisphere contralateral to the deprived eye (90.1 ± 3.6%, $n = 6$; Fig. 5*b*) compared with LTD in the ipsilateral hemisphere (72.6 ± 3.3%, $n = 5$).

We next asked whether LTD in layer 2/3 of mouse visual cortex is similarly disrupted by prior MD. LTD in layer 2/3 was significantly reduced (89.5 ± 3.6%, $n = 7$) in the visual cortex contralateral to the deprived eye compared with values obtained in the control ipsilateral hemispheres (73.8 ± 5.4%, $n = 6$; Fig. 5*a*) confirming previous findings in rats. Together, these data are consistent with the hypothesis that deprivation-induced synaptic depression *in vivo* utilizes, at least in part, the mechanisms of layer 4 (CA1-like) and layer 2/3 (CB1-mediated) LTD described here in brain slices.

Discussion

Modifications of synapses in the radial excitatory pathways afferent to layers 4 and 3 are responsible for the functional consequences of MD in the binocular region of visual cortex (19, 20). Motivated by a theoretical analysis of ocular dominance plasticity (21), LFS-LTD was introduced as an experimental paradigm that might help reveal the mechanisms (22). Here we show that, although activation of postsynaptic NMDARs by identical LFS protocols induces synaptic depression in both layers, there are significant laminar differences in the mechanism, and that LTD in layer 2/3 is mechanistically different than previously thought. These findings suggest new opportunities to dissect the individual contributions of plasticity in different layers to the ocular dominance shift in mice.

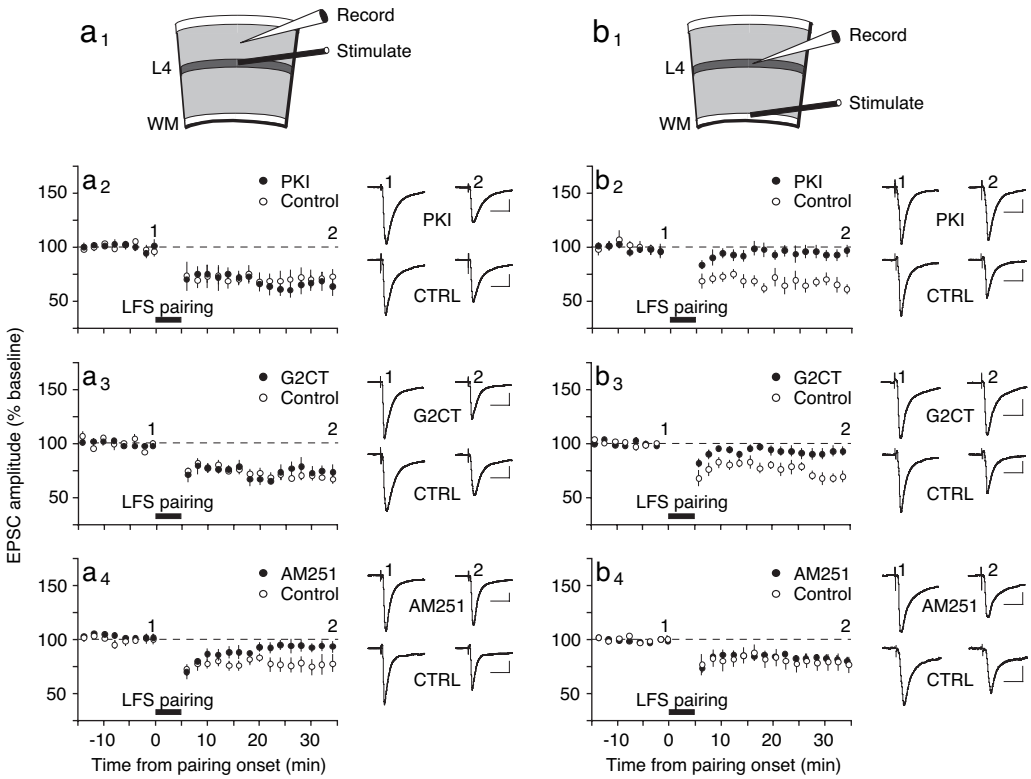

Fig. 3. Differences in pairing-induced LTD in layers 4 and 3 of visual cortex. (*a* and *b*) Displayed are grouped data time courses and representative sweeps from layers 2/3 (*a*) and 4 (*b*) recordings. LTD was challenged both extracellularly and intracellularly by a battery of antagonists, which highlight differences in LTD expression between layers. (a_1 and b_1) Schematic illustrations of recording configurations for layers 2/3 (a_1) and 4 (b_1). (a_2 and b_2) Intracellular loading of a PKA inhibitor PKI (6–22 amide, 10 μM) prevented LTD in layer 4 (b_2) but not in layer 2/3 (a_2). (a_3 and b_3) Intracellular loading of G2CT (10 μM), a peptide that interferes with regulated endocytosis of GluR2, also prevents LTD in layer 4 (b_3) but not layer 2/3 (a_3). (a_4 and b_4) Bath application of the CB1 antagonist AM251 (2 μM) had no effect on LTD in layer 4 (b_4) but largely prevented LTD in layer 2/3 (a_4). The *y* axis is EPSC amplitude normalized to a 15-min baseline period, with error bars indicating the SEM. The pairing protocol, denoted by the black bar, was administered at time 0 and lasted 5 min. The dashed horizontal line indicates no change from baseline responses. Sweep numbers (1 and 2) refer to averaged responses collected during the last 5 min of the baseline and postpairing periods. Stimulation artifacts were minimized for clarity. (Scale bars: 50 pA, 20 msec.) See Fig. 4 for statistical comparisons.

The first synaptic relay from the thalamus occurs in layer 4, which is a site of robust ocular dominance plasticity in mice (17, 23). Although extracellular stimulation of white matter activates these thalamic synapses (24), it is very likely that other sources of synaptic input are also recruited (e.g., recurrent collaterals). Considering this potential complication, it is remarkable that the LTD induced by our stimulation protocol was reliably blocked in all experiments by APV and postsynaptic inhibition of NMDAR channels, PKA, and AMPAR endocytosis. Thus, the large majority of synapses capable of expressing LTD on layer 4 neurons in response to LFS of the white matter use a mechanism that closely resembles what has been documented extensively in area CA1 of hippocampus (reviewed in ref. 5).

We hasten to point out that AMPAR endocytosis may not be the only mechanism for LTD in layer 4, particularly at intracortical synaptic connections. In synaptically coupled pairs of spiny stellate

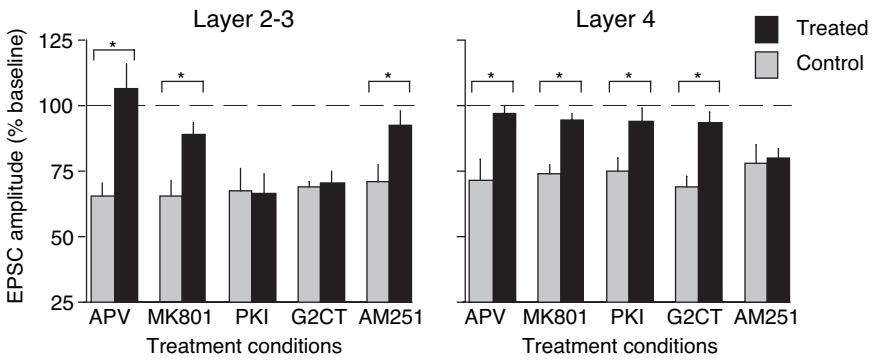

Fig. 4. Summary data comparing laminar differences in LTD. Filled bars represent mean ± SEM of EPSC 25–30 min after LFS (normalized to baseline) in neurons treated with the drugs indicated. Gray bars represent the effect of LFS in the interleaved vehicle-treated controls. The number of experiments in each group is indicated in the text. Note the consistency of LTD magnitude in all control experiments. APV and AM251 were bath-applied. MK801, PKI, and G2CT were loaded intracellularly. *, $P < 0.01$.

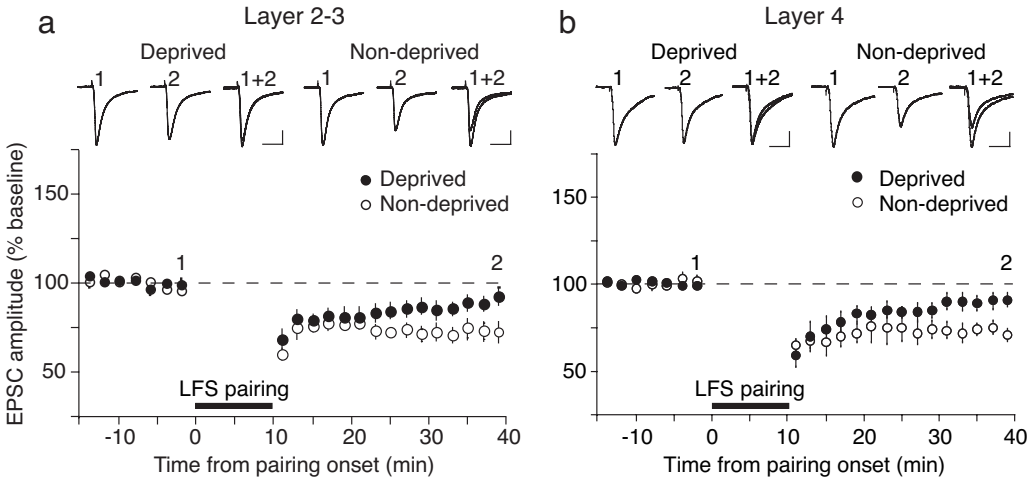

Fig. 5. Prior MD occludes subsequent LTD *ex vivo* in layers 2/3 and 4. (*a* and *b*) Male mice (P21–P28) were monocularly deprived for 3 days. On the third day, slices were obtained and whole-cell voltage-clamp recordings were performed from the binocular area of the deprived hemisphere (contralateral to the lid-sutured eye) or from the control hemisphere (ipsilateral to the lid-sutured eye). LTD was saturated by doubling the LFS-pairing protocol duration to 10 min. In both layers, robust LTD was induced in the control nondeprived hemisphere (*a*, layer 2/3, 73.8 ± 5.4%, $n = 6$; *b*, layer 4, 72.6 ± 3.3%, $n = 5$). In contrast, LTD was significantly occluded in the deprived hemisphere (*a*, layer 2/3, 89.5 ± 3.6%, $n = 7$, $P < 0.05$; *b*, layer 4, 90.1 ± 3.6%, $n = 6$; $P < 0.01$). 1 and 2 indicate 5-min periods for the averaging of EPSCs just before pairing (1) or at the conclusion of the recording session (2). Stimulus artifacts were minimized for clarity. (Scale bars: 50 pA, 20 msec.) The dashed line indicates no change from baseline responses. Recordings were performed with the experimenter blind to the visual history of the animal.

neurons in layer 4 of barrel cortex, for example, Egger *et al.* (25) reported a form of LTD induced with a spike-timing protocol that required activation of postsynaptic group II metabotropic glutamate receptors but not NMDARs (25). If these findings generalize to layer 4 of visual cortex (where most spiny neurons are pyramidal), they suggest that the diversity of mechanisms for LTD could parallel the diversity of sources of excitatory synaptic input to layer 4 neurons. Nonetheless, that prior MD decreases the magnitude (occludes) LTD of the radial input to layer 4 strongly supports the conclusion that naturally occurring synaptic depression similarly utilizes a mechanism of NMDAR-dependent endocytosis of AMPAR that is reliably elicited with LFS. Thus, our data support the previous conclusions of Heynen *et al.* (6) in rats and extend them to layer 4 of mice.

We were initially surprised to find that LTD induced in layer 2/3 by the same LFS protocol was insensitive to inhibitors of PKA and AMPAR endocytosis, but sensitive instead to antagonists of CB1 receptors. However, there is certainly ample precedent for laminar diversity (4) and endocannabinoid-dependent LTD in the brain (15, 26, 27). Indeed, paired recordings of synaptically coupled layer 5 neurons have revealed a form of LTD that requires the calcium-dependent release of endocannabinoid from the postsynaptic neuron that acts on presynaptic CB1 receptors to induce LTD (9, 28). Our findings in layer 2/3 could be explained by this mechanism if the calcium admitted by NMDARs during the LFS pairing protocol stimulates similar retrograde CB1 signaling. In any case, the finding that LFS-induced LTD in the layer 4 to layer 2/3 pathway is fundamentally different from that studied in CA1 challenges the underlying assumptions of a large number of previous studies. As Daw *et al.* (29) have pointed out, closer attention to laminar differences in LTD and ocular dominance plasticity may help resolve some of the lingering controversies in the field (see, e.g., ref. 30).

In contemporaneous experiments, Bender *et al.* (15, 31) showed in layer 2/3 neurons of rat barrel cortex that STD-LTD, also occluded by whisker deprivation, is similarly inhibited by APV and AM251. Thus, a reasonable conclusion is that LFS and spike-timing protocols induce layer 2/3 LTD in sensory cortex by a common mechanism that is also accessed by sensory deprivation. However, Bender *et al.* (15, 31) showed that intracellular MK801 (1 mM) had no effect on STD-LTD induction, whereas it was blocked by antagonists of metabotropic glutamate receptor 5 (mGluR5). They conclude that the relevant source of postsynaptic calcium for induction of STD-LTD is release from intracellular stores. These findings are in clear contrast with what has been observed with LFS-LTD. First, there is no effect of either group 1 mGluR antagonists or genetic deletion of mGluR5 on LFS-LTD in layer 2/3 of rat or mouse visual cortex (4, 32). Second, as we show here, LFS-LTD is reliably blocked by intracellular MK801 (500 μM). As a control for the possibility that MK801 might have leaked out of our recording pipette to affect presynaptic NMDARs implicated in STD-LTD, we repeated the experiments of Bender *et al.* (15, 31) using their spike-timing protocol in visual cortex of juvenile mice (Fig. 2). Consistent with their results, intracellular MK801 (500 μM) had no effect on STD-LTD that was reliably blocked by APV. These experiments confirm that MK801 applied through our pipettes does not meaningfully affect presynaptic NMDARs. Thus, we propose that postsynaptic NMDAR activation triggers the CB1-dependent LTD induced by LFS in layer 2/3 of mouse visual cortex.

Ocular dominance plasticity occurs in both layers 2/3 and 4. There is evidence in cats that plasticity in layer 2/3 occurs independently from that in layer 4 [e.g., late in the critical period (33)], and, further, that it may precede and actually be required for plasticity in layer 4 (34). Our finding that LTD within layer 4 is insensitive to CB1 antagonist is consistent with the fact that there is very little CB1 protein in this layer (35). Our results support the general notion of laminar differences in the mechanisms of deprivation-induced response depression and suggest an opportunity to disentangle their contributions to ocular dominance shifts. Because CB1 antagonists, like AM251, can completely block cannabinoid-dependent processes, including LTD in layers 3 and 5, they can potentially be used to pharmacologically isolate cannabinoid-independent mechanisms, like those used for LTD in layer 4, to assess their contributions to ocular dominance plasticity *in vivo*.

Materials and Methods

Slice Preparation for Whole-Cell Recordings. Slices of visual cortex (350 μm) from P21–P28 or P13–P15 C57BL/6 mice (Fig. 2) were

prepared as described (36). Briefly, mice were anesthetized, and the brains were rapidly removed and placed in ice-cold high-sucrose dissection solution and sectioned using a vibrating-blade microtome (Leica, Deerfield, IL; VT1000S). Slices containing primary visual cortex were transferred to a holding chamber with artificial cerebrospinal fluid containing 124 mM NaCl, 2.5 mM KCl, 2 mM $CaCl_2$, 1 mM $MgCl_2$, 1.23 mM NaH_2PO_4, 26 mM $NaHCO_3$, and 10 mM glucose. Slices were left undisturbed at 32°C for 1 h and subsequently stored at room temperature for the remainder of the day. Recordings were performed at 28–30°C. Individual neurons were visualized with IR-DIC optics by using a Nikon (Florham Park, NJ) microscope (E600FN) and 60× water-immersion objective.

Voltage-Clamp Recordings of LFS-LTD. Somatic whole-cell voltage-clamp recordings (37) were obtained from spiny pyramidal neurons in layer 2/3 and star pyramids in layer 4 by using patch pipettes filled with internal solution containing 107 mM D-gluconic acid, 107 mM CsOH, 5 mM QX-314-Cl^-, 0.2 mM EGTA, 20 mM Hepes, 3.7 mM NaCl, 4 mM Mg-ATP, 0.3 mM Na-GTP, and 10 mM Na-phosphocreatine with pH adjusted to 7.2. When filled with internal solution, pipette resistances were ≈5 MΩ. An empirically determined liquid-junction potential (approximately −12 mV) was corrected (38). EPSCs were elicited with a two-contact cluster electrode (FHC, Bowdoin, ME) placed in layer 4 for layer 2/3 recordings or in white matter for layer 4 recordings. Test stimuli (100 μsec) were delivered at 0.05 Hz. The test holding potential was −65 mV. LFS-LTD was induced by pairing 1-Hz presynaptic stimulation with a brief (100-msec) postsynaptic-step depolarization from −65 to −45 mV for each of the 300 or 600 pulses (Fig. 5). Each presynaptic stimulation occurred midway (50 msec) into the step depolarization. Series resistance was estimated every fifth sweep by measuring the peak of the capacity transient elicited by a 5-mV hyperpolarizing pulse from −65 to −70 mV, and experiments were discarded if this value changed by >20% during the recording. Data acquisition and analysis were performed on a personal computer running pClamp 9.2 (Molecular Devices, Sunnyvale, CA).

Current-Clamp Recordings of STD-LTD. The internal solution consisted of 100 mM K-gluconate/20 mM KCl/4 mM Mg-ATP/0.3 mM GTP/10 mM phosphocreatine/10 mM Hepes, pH 7.3. Pipette resistances were ≈6 MΩ when filled with internal solution. For current-clamp recordings of STD-LTD (Fig. 2), test stimuli (0.3 msec) were delivered at 0.1 Hz, and STD-LTD was induced by pairing presynaptic stimulation ≈25 msec after a postsynaptic spike repeated for 100 times at 0.2 Hz. The postsynaptic spikes were elicited by injecting a depolarizing current (0.2 msec in duration) and were of sufficient magnitude to yield an action potential for every trial. Picrotoxin (20 μM) was present for the duration of the STD-LTD experiment. Recordings were considered acceptable if membrane potentials were maintained between −55 and −70 mV. EPSPs were acquired and analyzed on a Macintosh (Apple, Cupertino, CA) computer by using custom routines written in Igor (WaveMetrics, Lake Oswego, OR).

Reagents. The following reagents were prepared as stock solutions in distilled water, stored at −80°C, and diluted 1:1,000 on the day of use: 100 μM APV (Calbiochem, La Jolla, CA), 10 μM PKI (Calbiochem); 10 μM G2CT peptide (KRMKLNINPS; Massachusetts Institute of Technology, CCR Biopolymers Laboratory, Cambridge, MA); 500 μM MK801 (Sigma, St. Louis, MO). For experiments involving intracellular loading of MK801, a cell was patched, and then the slice was rinsed for 15–20 min such that a minimum of 25–30 min had elapsed before induction of LFS- or STD-LTD to ensure clearance of MK801 from the extracellular milieu. Biocytin 0.2–0.4% (wt/vol; Molecular Probes, Eugene, OR) was included in pipette solutions for post hoc examination. Biocytin was detected with streptavidin AlexaFluor 488 (Molecular Probes) and imaged on a confocal microscope (Olympus, Melville, NY). AM251 (2 μM; Tocris Cookson, Bristol, U.K.) was diluted 1:40,000 in DMSO and also contained BSA at a final concentration of 0.5 mg/ml to prevent AM251 from adhering to the perfusion line. Lid suture for MD was performed as described (6, 17).

Statisics. The peak amplitude of the EPSC or EPSP was measured. A 15-min (LFS-LTD) or 10-min (STD-LTD) baseline period just before the respective conditioning protocol was averaged and compared with the average of the final 5 min of the recording. Data are displayed as percent baseline ± SEM. Statistics were computed by using StatView 5 (SAS Institute, Cary, NC). Statistical differences were confirmed by one-way analysis of variance with Fisher's probable least-squares difference comparisons among groups, and data were considered statistically significant at $P < 0.05$.

This research was supported by the National Eye Institute and Howard Hughes Medical Institute.

1. Gilbert CD, Wiesel TN (1983) *Prog Brain Res* 58:209–218.
2. McAllister AK, Usrey WM (2003) *Nat Neurosci* 6:787–788.
3. Kirkwood A, Dudek SM, Gold JT, Aizenman CD, Bear MF (1993) *Science* 260:1518–1521.
4. Rao Y, Daw NW (2004) *J Neurophysiol* 92:2652–2658.
5. Malenka RC, Bear MF (2004) *Neuron* 44:5–21.
6. Heynen AJ, Yoon BJ, Liu CH, Chung HJ, Huganir RL, Bear MF (2003) *Nat Neurosci* 6:854–862.
7. Markram H, Lubke J, Frotscher M, Sakmann B (1997) *Science* 275:213–215.
8. Shouval HZ, Bear MF, Cooper LN (2002) *Proc Natl Acad Sci USA* 99:10831–10836.
9. Sjostrom PJ, Turrigiano GG, Nelson SB (2003) *Neuron* 39:641–654.
10. Dudek SM, Friedlander MJ (1996) *Neuron* 16:1–20.
11. Kirkwood A, Bear MF (1994) *J Neurosci* 14:3404–3412.
12. Berretta N, Jones RS (1996) *Neuroscience* 75:339–344.
13. Arvanian VL, Mendell LM (2001) *J Neurophysiol* 86:123–129.
14. Humeau Y, Shaban H, Bissiere S, Luthi A (2003) *Nature* 426:841–845.
15. Bender VA, Bender KJ, Brasier DJ, Feldman DE (2006) *J Neurosci* 26:4166–4177.
16. Lee SH, Liu L, Wang YT, Sheng M (2002) *Neuron* 36:661–674.
17. Frenkel MY, Bear MF (2004) *Neuron* 44:917–923.
18. Philpot BD, Espinosa JS, Bear MF (2003) *J Neurosci* 23:5583–5588.
19. Daw N (1994) *Invest Opthalmol Visual Sci* 35:4168–4179.
20. Bear MF, Rittenhouse CD (1999) *J Neurobiol* 41:83–91.
21. Bienenstock EL, Cooper LN, Munro PW (1982) *J Neurosci* 2:32–48.
22. Bear MF (2003) *Philos Trans R Soc London B* 358:649–655.
23. Tagawa Y, Kanold PO, Majdan M, Shatz CJ (2005) *Nat Neurosci* 8:380–388.
24. Aizenman C, Kirkwood A, Bear M (1996) *Cereb Cortex* 6:751–758.
25. Egger V, Feldmeyer D, Sakmann B (1999) *Nat Neurosci* 2:1098–1105.
26. Robbe D, Kopf M, Remaury A, Bockaert J, Manzoni OJ (2002) *Proc Natl Acad Sci USA* 99:8384–8388.
27. Gerdeman GL, Ronesi J, Lovinger DM (2002) *Nat Neurosci* 5:446–451.
28. Sjostrom PJ, Turrigiano GG, Nelson SB (2004) *J Neurophysiol* 92:3338–3343.
29. Daw N, Rao Y, Wang XF, Fischer Q, Yang Y (2004) *Vision Res* 44:3377–3380.
30. Renger JJ, Hartman KN, Tsuchimoto Y, Yokoi M, Nakanishi S, Hensch TK (2002) *Proc Natl Acad Sci USA* 99:1041–1046.
31. Bender KJ, Allen CB, Bender VA, Feldman DE (2006) *J Neurosci* 26:4155–4165.
32. Sawtell NB, Huber KM, Roder JC, Bear MF (1999) *J Neurophysiol* 82:3594–3597.
33. Daw NW, Fox K, Sato H, Czepita D (1992) *J Neurophysiol* 67:197–202.
34. Trachtenberg JT, Trepel C, Stryker MP (2000) *Science* 287:2029–2032.
35. Marsicano G, Lutz B (1999) *Eur J Neurosci* 11:4213–4225.
36. Philpot BD, Sekhar AK, Shouval HZ, Bear MF (2001) *Neuron* 29:157–169.
37. Hamill OP, Marty A, Neher E, Sakmann B, Sigworth FJ (1981) *Pflügers Arch* 391:85–100.
38. Neher E (1992) *Methods Enzymol* 207:123–131.